Optical Spectroscopic Studies of the Metal-Insulator Transition Driven by All-In–All-Out Magnetic Ordering in 5*d* Pyrochlore $Cd_2Os_2O_7$

C. H. Sohn,[1,2] Hogyun Jeong,[1] Hosub Jin,[1,2,3] Soyeon Kim,[1,2] L. J. Sandilands,[1,2] H. J. Park,[1,2] K. W. Kim,[4] S. J. Moon,[5] Deok-Yong Cho,[6] J. Yamaura,[7] Z. Hiroi,[8] and T. W. Noh[1,2]

[1]*Center for Correlated Electron Systems, Institute for Basic Science (IBS), Seoul 08826, Republic of Korea*
[2]*Department of Physics and Astronomy, Seoul National University (SNU), Seoul 08826, Republic of Korea*
[3]*Department of Physics, Ulsan National Institute of Science and Technology, Ulsan 44919, Republic of Korea*
[4]*Department of Physics, Chungbuk National University, Cheongju, Chungbuk 28644, Republic of Korea*
[5]*Department of Physics, Hanyang University, Seoul 04763, Republic of Korea*
[6]*Department of Physics, Chonbuk National University, Jeonju 54896, Republic of Korea*
[7]*Materials Research Center for Element Strategy, Tokyo Institute of Technology, Kanagawa 226-8503, Japan*
[8]*ISSP, University of Tokyo, Kashiwa 277-8581, Japan*

(Received 10 May 2015; published 28 December 2015)

We investigated the metal-insulator transition (MIT) driven by all-in–all-out (AIAO) antiferromagnetic ordering in the 5*d* pyrochlore $Cd_2Os_2O_7$ using optical spectroscopy and first-principles calculations. We showed that the temperature evolution in the band-gap edge and free carrier density were consistent with rigid upward (downward) shifts of electron (hole) bands, similar to the case of Lifshitz transitions. The delicate relationship between the band gap and free carrier density provides experimental evidence for the presence of an AIAO metallic phase, a natural consequence of such MITs. The associated spectral weight change at high energy and first-principles calculations further support the origin of the MIT from the band shift near the Fermi level. Our data consistently support that the MIT induced by AIAO ordering in $Cd_2Os_2O_7$ is not close to a Slater type but instead to a Lifshitz type.

DOI: 10.1103/PhysRevLett.115.266402 PACS numbers: 71.30.+h, 78.20.-e, 78.30.-j

Since Mott [1], metal-insulator transitions (MITs) and related magnetism have long been a central theme in correlated electron systems including manganites and curates [2]. Recently, MITs and antiferromagnetic ordering in 5*d* pyrochlores, $A_2B_2O_7$ (B = Ir, Os), have received much attention due to their strong correlation and the key role they play in novel phases. The MITs in these compounds [3–8] reportedly are prompted by the emergence of magnetic ordering. Such magnetism-driven MITs are expected to induce exotic phenomena, including a Weyl semimetal [9–12] and quantum criticality [13] in rare-earth pyrochlore iridates. However, questions remain as to how magnetic ordering induces MITs in 5*d* pyrochlores.

The peculiar antiferromagnetic structure in 5*d* pyrochlores makes the MITs distinct from the Slater type [14], a well-known magnetic-driven MIT. In the original Slater picture, collinear antiferromagnetic ordering induces a doubling of the lattice periodicity, resulting in a BCS-like band gap at the folded zone boundaries. However, recent studies support that the magnetic ground states in 5*d* pyrochlores are noncollinear all-in–all-out (AIAO) magnetic orderings [9–11,15–17], where all spins in transition metal ions align inward or outward of tetrahedra. Since AIAO ordering maintains the unit cell of pyrochlores, a new paradigm beyond the Slater picture is essential to understanding MITs in 5*d* pyrochlores.

$Cd_2Os_2O_7$ is a good candidate for the study of such MITs, in that it shows a continuous MIT at an antiferromagnetic ordering temperature T_N (= 227 K) [18,19]. Until its magnetic ground state was revealed, this material was best known as one of a few examples of a Slater insulator [20]. However, recent experimental [19,21] and theoretical [22,23] results showed that the magnetic ground state in $Cd_2Os_2O_7$ is AIAO ordering. Investigations on $Cd_2Os_2O_7$ should provide an understanding of how AIAO ordering causes MITs in 5*d* pyrochlores.

In this Letter, we report on the detailed temperature (T) evolution of the optical spectra of $Cd_2Os_2O_7$ to reveal how the emergence of AIAO ordering affects the electronic structure and induces the MITs. The absorption edge analyses suggest the Lifshitz-type MIT where a rigid shift of the bands away from the Fermi level E_F gradually annihilates the Fermi surface [22,24]. The model based on the Lifshitz-type MIT reproduces the delicate relationship between the band gap and plasma frequency well, thereby providing evidence for the existence of an AIAO metal, the inevitable intermediate state in such a MIT. This was further corroborated by an analysis of the interband transition using *ab initio* results.

We measured near-normal reflectance spectra of high-quality single-crystal $Cd_2Os_2O_7$ [25] from 7 meV to 1 eV using a Bruker IFS 66 v/s Fourier transform infrared spectrometer and an *in situ* gold evaporation technique [26]. The optical constants between 0.74 and 5 eV were obtained directly using a V-VASE ellipsometer (J. A. Woollam Co.). Kramers-Kronig analysis was then applied

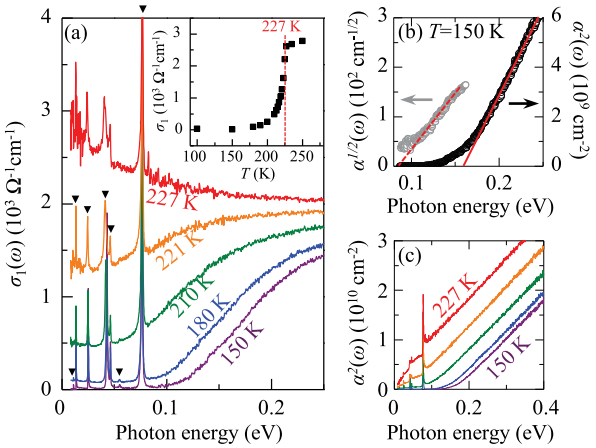

FIG. 1 (color online). (a) T-dependent $\sigma_1(\omega)$ below 0.25 eV. The solid triangles highlight the phonons. The inset in (a) shows T-dependent $\sigma_1(\omega)$ at $\hbar\omega = 20$ meV. (b) $\alpha^2(\omega)$ and $\alpha^{1/2}(\omega)$ at 150 K. The solid and dashed lines are extrapolation lines for two spectra. (c) T-dependent $\alpha^2(\omega)$.

to obtain the optical constants below 0.74 eV. For the low-frequency extrapolation, we used the Hagen-Rubens relation (a constant) above (below) 180 K. A two-point high-energy anchoring method [27] was used to minimize the uncertainty in the Kramers-Kronig analysis.

A clear MIT is observed in the real part of the optical conductivity, $\sigma_1(\omega)$, similar to the previous report [20]. Figure 1(a) shows the T-dependent $\sigma_1(\omega)$ below 0.25 eV. Below 150 K, the clear band-gap edge and no spectral weight (SW) below the gap indicate a robust insulating phase. The seven sharp peaks correspond to infrared active phonons of the pyrochlores [28]. With increasing T, the band-gap-edge energy decreases, and SW below the band gap, which corresponds to the Drude response of the free carriers, emerges. To see the evolution of the free carriers, we plotted $\sigma_1(\omega)$ at $\hbar\omega = 20$ meV as a function of T in the inset in Fig. 1(a). The evolution in $\sigma_1(\omega)$ becomes significant as T approaches 227 K and negligible above T. This T is identical with the known T_N in previous experiments [18,19], indicating that the MIT in $Cd_2Os_2O_7$ is strongly correlated with AIAO ordering.

The band-gap edge at low T shows the direct and indirect transitions, giving information about the electronic structures of $Cd_2Os_2O_7$. Figure 1(b) shows the square and square root of the absorption coefficient $\alpha(\omega)$ at 150 K. In direct transitions, $\alpha(\omega)$ is proportional to $m_r^{3/2}\sqrt{\hbar\omega - 2\Delta_D}$, where m_r ($2\Delta_D$) is the reduced mass of conduction and valence bands (the optical direct gap) [29]. The good linearity in $\alpha^2(\omega)$ indicates that most SW near the band-gap edge comes from a direct transition. $2\Delta_D$ is 158 meV, obtained from the linear extrapolation of $\alpha^2(\omega)$ (a solid line). However, $\alpha^2(\omega)$ clearly deviates from linear behavior at a low energy, which could result from indirect transitions. The indirect gap (i.e., charge gap) $2\Delta_C$ is estimated roughly to be about 80 meV in the linear extrapolation of $\alpha^{1/2}(\omega)$ (dashed line) [29], although an accurate value is obscure due to the lack of information about the phonon energy involved. These analyses illustrate that the electronic structure of $Cd_2Os_2O_7$ has direct and indirect transitions; their energy difference is on the order of tens of meV.

The T evolutions in $\alpha^2(\omega)$ reveal that the band gap closing through MITs occurs without significant band-dispersion change, providing the first piece of evidence for a Lifshitz-type MIT. Figure 1(c) shows $\alpha^2(\omega)$ from 150 to 227 K. Notably, although $\alpha^2(\omega)$ spectra shift to a lower energy with increasing T, their slopes remain almost the same. Since the slope of $\alpha^2(\omega)$ is proportional to m_r^3 [29], the unvarying slope indicates that the MIT involves a rigid shift of the conduction and valence bands without a strong band-dispersion change. We will show that such a rigid shift can self-consistently explain the T-dependent $\sigma_1(\omega)$.

To quantify the T evolution of$\sigma_1(\omega)$, we fitted it using a minimum model. Seven Lorentz oscillators, a single Drude term, and a critical point M_0 (CPM_0) model [30] were used for phonons, for the free carrier response, and for the direct transition, respectively. Since indirect transitions are orders of magnitude weaker than direct transitions [29], we did not consider the indirect transitions here. Figures 2(a) and 2(b) exhibit $\sigma_1(\omega)$ and the real part of the dielectric constant $\epsilon_1(\omega)$ at 200 K and their fitting results. Our minimal model fits both $\sigma_1(\omega)$ and $\epsilon_1(\omega)$ well for all T, validating our fitting model. However, due to the large overlap between the Drude response and band-gap edge at high T, the fitting error bars became significant above 219 K. Figure 2(c) shows $2\Delta_D(T)$ (solid square) from the CPM_0 model [31] and the square of the plasma frequency (solid triangle), $\omega_p^2(T) = 8\int_0^\infty \sigma_{1\,\mathrm{Drude}}(\omega, T)d\omega$ from the Drude model, which is proportional to n/m^*, where n (m^*) is the free carrier density (effective mass).

The relationship between $\omega_p^2(T)$ and $\Delta_D(T)$ below T_N is inconsistent with that of thermally excited carriers, providing the second piece of evidence for a Lifshitz-type MIT. Although the MIT starts to occur at 227 K, Fig. 2(c) shows finite values of $\omega_p^2(T)$ until 180 K. In a Slater or density-wave picture, at least a small charge gap should open at the transition T and only thermally excited carriers contribute to the finite $\omega_p^2(T)$ below the T. Then, $\omega_p^2(T)$ is proportional to $e^{-\Delta_D(T)/k_BT}$ [33] with constant m^* demonstrated by $\alpha^2(\omega)$ and extended Drude model analyses [31]. The solid circle in Fig. 2(d) is $\omega_p^2(T)$ on a log scale as a function of $\Delta_D(T)/k_BT$. The gradient of $\omega_p^2(T)$ deviates from exponential behaviors (dashed line), especially above 210 K, indicating that remaining carriers cannot be explained solely by thermal excitation.

The observed inconsistency with thermal carriers can be explained within a Lifshitz-type MIT model described in Fig. 2(e). Above T_N, the system is metallic with the same number of electrons and holes due to the even number of electrons in the unit cell. If T falls below T_N, the emergence of AIAO ordering induces upward or downward shifts of

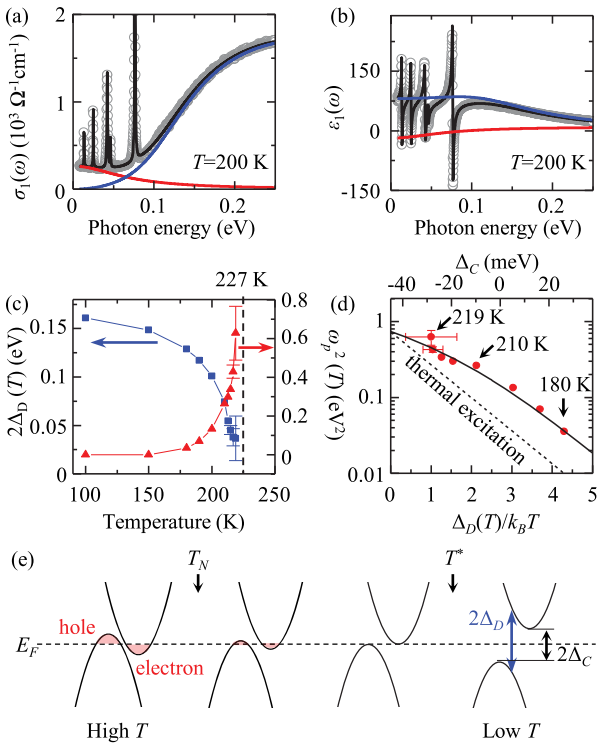

FIG. 2 (color online). (a) $\sigma_1(\omega)$ and (b) $\epsilon_1(\omega)$ at 200 K. The open circles are experimental data; the solid lines show the fitting results. The red and blue lines correspond to the Drude and CPM_0 models, respectively. (c) $\Delta_D(T)$ and $\omega_p^2(T)$. The error bars indicate the 95% confidence interval. Error bars smaller than the symbol size are omitted. (d) $\omega_p^2(T)$ as a function of $\Delta_D(T)/k_BT$. The solid circles are experimental data, and the solid line is the best fitting result with the model. The dashed line shows the case of the thermal excitation limit. The Δ_C values that correspond to the solid line are shown on the top axis. (e) A model band structure describing a Lifshitz-type MIT.

bands, gradually annihilating the Fermi surface. With further decrease in T, the electron and hole pockets disappear completely below a certain T, T^*, resulting in a robust insulating phase. Note that, since intrinsic free carriers can exist even below T_N in this MIT, AIAO metallic states should be located between paramagnetic metallic and AIAO insulating phases.

Within this model, the relationship between $\Delta_D(T)$ and $\omega_p^2(T)$ was calculated using the following equation:

$$\Delta_D(T) = \Delta_C(T) + C, \tag{1}$$

$$\omega_p^2(T) = A\int_{\Delta_C(T)}^{\infty} \frac{\sqrt{\hbar\omega - \Delta_C(T)}}{e^{\hbar\omega/k_BT}+1}\, d\omega, \tag{2}$$

where A and C are the normalization factor and energy difference between Δ_D and Δ_C, respectively. We fixed $T =$ 200 K as we focused on a narrow T region from 180 to 219 K. For simplicity, we assumed that both the valance and conduction bands were 3D parabolic with the same m, although previous Hall measurements revealed that m of electrons is slightly smaller than that of holes [34]. We found that calculations without these assumptions gave similar results [31]. The denominator (numerator) in Eq. (2) was derived from the Fermi-Dirac distribution (density of states of a 3D system). The metallic state is naturally accounted for when Δ_C becomes negative. If $\Delta_C(T)$ in Eq. (2) is substituted with $\Delta_D(T) - C$ using Eq. (1), we can calculate the relationship between $\omega_p^2(T)$ and $\Delta_D(T)$. Since A gives only an offset in Fig. 2(d), C is the single fitting parameter in this model.

Despite its simplicity, the above model captures most of the subtle relationship between the $\omega_p^2(T)$ and $\Delta_D(T)$. In Fig. 2(d), the solid line is the simulated $\omega_p^2(T)$ as a function of $\Delta_D(T)/k_BT$ using the model with $C = 45$ meV. The good agreement between the experimental data and model calculations implies that the MIT observed is close to the case illustrated in Fig. 2(e) [35]. Furthermore, the C value we obtained is consistent with the energy difference between the direct and indirect gaps in Fig. 1(b), being on the order of a few tens of meV. A constant offset of 45 meV is also supported by an analysis of the charge gap extracted from transport [31].

The gradient change of $\omega_p^2[\Delta_D(T)/k_BT]$ in Fig. 2(d) can be interpreted in the presence of the AIAO metallic phase in Fig. 2(e). Since Δ_D at 210 K is 32 meV, the 45 meV energy difference between $\Delta_D(T)$ and $\Delta_C(T)$ indicates that the charge gap remains closed until 210 K, when a smooth gradient change of $\omega_p^2[\Delta_D(T)/k_BT]$ occurs. Specifically, the decrease in $\omega_p^2(T)$ with increasing $\Delta_D(T)/k_BT$ becomes faster below 210 K. This can be explained in terms of the different origins of the free carriers. Before the charge gap opens, n is close to the number of intrinsic carriers proportional to $[-\Delta_C(T)]^{3/2} = [C - \Delta_D(T)]^{3/2}$ (Fermi surface volume). After the charge gap opens, however, n originates from the thermal excitations and is roughly exponential in $\Delta_D(T)/k_BT$. Since ω_p^2 tends to show power law (exponential) behavior with $\Delta_D(T)/k_BT$ before (after) the charge gap opens, the gradient change in $\omega_p^2[\Delta_D(T)/k_BT]$ at 210 K in Fig. 2(d) can be interpreted in a charge gap opening at T^* in Fig. 2(e), thereby implying the existence of an AIAO metallic phase between 210 and 227 K. Note that, since the transition at T^*, from the AIAO metal to the AIAO insulator, is a crossover [36], it is difficult to observe the signatures of the AIAO metallic phase in previous experiments including resistivity or heat capacity [18,19].

Further evidence for a Lifshitz-type MIT can be found in the high-energy $\sigma_1(\omega)$, because it reflects the electronic structure change through the MIT. Figure 3(a) shows $\sigma_1(\omega)$ over the full range of measured energies at four different T. It is evident that missing low-energy SWs through the MIT transfer to high-energy regions. To see the SW transfer more clearly, we calculated the SW using the three

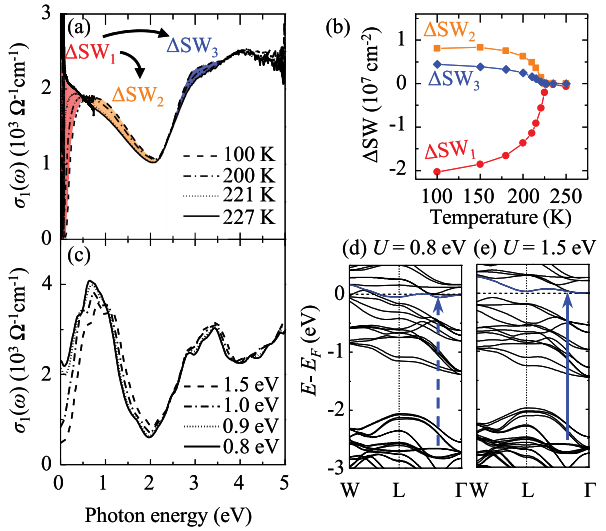

FIG. 3 (color online). (a) $\sigma_1(\omega)$ with four different T. (b) T-dependent SW changes in three different energy regions. (c) $\sigma_1(\omega)$ from LDA calculations with four different U values. Band structures with (d) $U = 0.8$ and (e) 1.5 eV. The dashed and solid arrows in (d) and (e) indicate forbidden and allowed optical transitions corresponding to the SW_3 region, respectively.

isosbestic points at 0.5, 2.4, and 3.7 eV, where all of the spectra meet [38], as boundaries: $SW_1 = \int_{0\text{ eV}}^{0.5\text{ eV}} \sigma_1(\omega)d\omega$, $SW_2 = \int_{0.5\text{ eV}}^{2.4\text{ eV}} \sigma_1(\omega)d\omega$, and $SW_3 = \int_{2.4\text{ eV}}^{3.7\text{ eV}} \sigma_1(\omega)d\omega$. Figure 3(b) shows the change in the SWs with respect to the 227 K data (ΔSW_1, ΔSW_2, and ΔSW_3). The clear features at 227 K show that the emergence of AIAO ordering induces SW transfer from SW_1 to SW_2, SW_3, and even higher energy regions. Such a SW transfer over a wide energy range is unexpected, because $2\Delta_D$ at 100 K is only about 0.17 eV.

To understand the unusual high-energy SW transfer, we performed local-density approximation (LDA) calculations. We solved the Kohn-Sham equation [39] with a primitive cell of the experimental crystal geometry [18]. We specified the basis set expansion by $K_{\max}R_{\text{MT}} = 8$. Spin-orbit coupling and electron correlation energy U were considered. We integrated an $8 \times 8 \times 8k$ grid using the Methfessel-Paxton method with 300 K broadening. The linear response $\sigma_1(\omega)$ was calculated using the Kubo formalism, tailored to augmented plane waves [40]. Since the intraband transitions were not considered, it inevitably underestimated the low-energy spectra compared with experiments. The finite values at zero energy in calculated $\sigma_1(\omega)$ come from an artificial thermal broadening effect.

To see the effect of AIAO ordering on the electronic structure at finite T, several theoretical calculations for $5d$ pyrochlores have used LDAs with different U, valid in the mean-field level [10,11,22,23]. Although AIAO ordering and enhancement of U cannot be exactly the same, we can approximately see the effect of AIAO ordering on the electronic structure of $5d$ pyrochlores using this method. Figure 3(c) shows $\sigma_1(\omega)$ from LDA calculations with four different U values. The overall shape and SW transfer in our optical spectra are well reproduced in Fig. 3(c), implying that AIAO ordering indeed changes the electronic structure in a similar way with enhancement of U. In addition, as shown in the calculated band structures with $U = 0.8$ and 1.5 eV [Figs. 3(d) and 3(e)], enhancement of U moves the valence (conduction) bands downward (upward) without significant band dispersion change, consistent with a Lifshitz-type MIT.

The LDA results reveal that the Lifshitz-type MIT described in Fig. 2(e) could explain the observed high-energy SW transfer. At $U = 0.8$ eV, the presence of electron and hole pockets indicates that the system is metallic. If we increase U (develop AIAO ordering), the bands near E_F move upward and downward, and the electron and hole pockets gradually disappear. As a result, although the total occupied and unoccupied density of states should remain the same (charge conservation), the occupied and unoccupied density of states at each k point will be different. Since Δk is 0 in optical transitions and its selection rule varies depending on k, such changes can affect even high-energy optical transitions. For example, the enhancement of SW_3 is simply explained by the vanishing of an electron pocket along the $L - \Gamma$ points as follows [31]. In Fig. 3(d), the optical transition from higher binding energies to unoccupied states along the $L - \Gamma$ points (dashed arrow) should be suppressed due to the small electron pocket. However, as shown in Fig. 3(e), such transitions become allowed due to the vanishing of the electron pocket through MITs, resulting in an enhancement of SW_3.

Comparing the MITs in $Cd_2Os_2O_7$ and $5d$ pyrochlore rare-earth iridates is worthwhile. In the calculated phase diagram of $5d$ pyrochlore iridates [11], metal, semimetal, and topological insulator were predicted at $U = 0$. As U increases (e.g., magnetic order onsets), the metal undergoes sequential transitions to an AIAO metal and then an AIAO insulator, consistent with our result. Therefore, although the band structures are different from each other, our understanding of the MIT in $Cd_2Os_2O_7$ could be applied to many other $5d$ pyrochlore systems. In addition, the good agreement between our results and theoretical predictions increases the possibilities of the exotic phenomena [11,13] in related materials. Thus, experiments on other $5d$ pyrochlores are strongly recommended.

In summary, MITs in $Cd_2Os_2O_7$ were investigated by optical spectroscopy and first-principles calculations. The T-dependent band-gap edge, free carrier densities, and SW at high energy consistently support that the MIT is close to Lifshitz type. Our results demonstrate how AIAO ordering induces MITs and lays the groundwork for unique phenomena in $5d$ pyrochlores.

We thank E. G. Moon, K. S. Burch, and Y. B. Kim for helpful discussions. This work was supported by IBS-R009-D1. S. J. M. and D.-Y. C.was supported by

Basic Science Research Program through the National Research Foundation of Korea (NRF) funded by the Ministry of Science, ICT and Future Planning (NRF-2014R1A2A1A11054351 and NRF-2015R1C1A1A02037514, respectively).

[1] N. F. Mott, Proc. Phys. Soc. London Sect. A **62**, 416 (1949).
[2] M. Imada, A. Fujimori, and Y. Tokura, Rev. Mod. Phys. **70**, 1039 (1998).
[3] K. Matsuhira, M. Wakeshima, R. Nakanishi, T. Yamada, A. Nakamura, W. Kawano, S. Takagi, and Y. Hinatsu, J. Phys. Soc. Jpn. **76**, 043706 (2007).
[4] K. Matsuhira, M. Wakeshita, Y. Hinatsu, and S. Takagi, J. Phys. Soc. Jpn. **80**, 094701 (2011).
[5] M. Sakata, T. Kagayama, K. Shimizu, K. Matsuhira, S. Takagi, M. Wakeshima, and Y. Hinatsu, Phys. Rev. B **83**, 041102(R) (2011).
[6] J. J. Ishikawa, E. C. T. O'Farrell, and S. Nakatsuji, Phys. Rev. B **85**, 245109 (2012).
[7] F. F. Tafti, J. J. Ishikawa, A. McCollam, S. Nakatsuji, and S. R. Julian, Phys. Rev. B **85**, 205104 (2012).
[8] H. Guo, K. Matsuhira, I. Kawasaki, M. Wakeshima, Y. Hinatsu, I. Watanabe, and Z.-A. Xu, Phys. Rev. B **88**, 060411(R) (2013).
[9] X. Wan, A. M. Turner, A. Vishwanath, and S. Y. Savrasov, Phys. Rev. B **83**, 205101 (2011).
[10] W. Witczak-Krempa and Y. B. Kim, Phys. Rev. B **85**, 045124 (2012).
[11] W. Witczak-Krempa, A. Go, and Y. B. Kim, Phys. Rev. B **87**, 155101 (2013).
[12] K. Ueda, J. Fujioka, Y. Takahashi, T. Suzuki, S. Ishiwata, Y. Taguchi, and Y. Tokura, Phys. Rev. Lett. **109**, 136402 (2012).
[13] L. Savary, E. G. Moon, and L. Balents, Phys. Rev. X **4**, 041027 (2014).
[14] J. C. Slater, Phys. Rev. **82**, 538 (1951).
[15] S. Zhao, J. M. Mackie, D. E. MacLaughlin, O. O. Bernal, J. J. Ishikawa, Y. Ohta, and S. Nakatsuji, Phys. Rev. B **83**, 180402(R) (2011).
[16] K. Tomiyasu, K. Matsuhira, K. Iwasa, M. Watahiki, S. Takagi, M. Wakeshima, Y. Hinatsu, M. Yokoyama, K. Ohoyama, and K. Yamada, J. Phys. Soc. Jpn. **81**, 034709 (2012).
[17] H. Sagayama, D. Uematsu, T. Arima, K. Sugimoto, J. J. Ishikawa, E. O'Farrell, and S. Nakatsuji, Phys. Rev. B **87**, 100403(R) (2013).
[18] D. Mandrus, J. R. Thompson, R. Gaal, L. Forro, J. C. Bryan, B. C. Chakoumakos, L. M. Woods, B. C. Sales, R. S. Fishman, and V. Keppens, Phys. Rev. B **63**, 195104 (2001).
[19] J. Yamaura, K. Ohgushi, H. Ohsumi, T. Hasegawa, I. Yamauchi, K. Sugimoto, S. Takeshita, A. Tokuda, M. Takata, M. Udagawa, M. Takigawa, H. Harima, T. Arima, and Z. Hiroi, Phys. Rev. Lett. **108**, 247205 (2012).
[20] W. J. Padilla, D. Mandrus, and D. N. Basov, Phys. Rev. B **66**, 035120 (2002).
[21] S. Tardif, S. Takeshita, H. Ohsumi, J. Yamaura, D. Okuyama, Z. Hiroi, M. Takata, and T. Arima, Phys. Rev. Lett. **114**, 147205 (2015).
[22] H. Shinaoka, T. Miyake, and S. Ishibashi, Phys. Rev. Lett. **108**, 247204 (2012).
[23] G.-W. Chern and C. D. Batista, Phys. Rev. Lett. **107**, 186403 (2011).
[24] I. M. Lifshitz, Sov. Phys. JETP **11**, 1130 (1960).
[25] J. Yamaura, H. Ohsumi, K. Sugimoto, S. Tsutsui, Y. Yoda, S. Takeshita, A. Tokuda, S. Kitao, M. Kurokuzu, M. Seto, I. Yamauchi, K. Ohgushi, M. Takigawa, T. Arima, and Z. Hiroi, J. Phys. Conf. Ser. **391**, 012112 (2012).
[26] C. C. Homes, M. Reedyk, D. A. Cradles, and T. Timusk, Appl. Opt. **32**, 2976 (1993).
[27] D. Y. Smith, in *Handbook of Optical Constants of Solids*, edited by E. D. Palik (Academic, San Diego, 1985).
[28] N. T. Vandenborre, E. Husson, and H. Brusset, Spectrochim. Acta, Part A **37**, 113 (1981).
[29] P. Y. Yu and M. Cardona, *Fundamentals of Semiconductors*, 3rd ed. (Springer, New York, 2005).
[30] S. Adachi, Phys. Rev. B **35**, 7454 (1987).
[31] See Supplemental Material at http://link.aps.org/supplemental/10.1103/PhysRevLett.115.266402 for comparison between the optical direct gap and BCS gap, extended Drude model analyses, Lifshitz model calculation, Resistivity, difference between optical and charge gap, and k-resolved optical transition analyses, which includes Ref. [32].
[32] G. Burns, *Solid State Physics* (Academic, New York, 1985).
[33] I. Lo Vecchio, A. Perucchi, P. Di Pietro, O. Limaj, U. Schade, Y. Sun, M. Arai, K. Yamaura, and S. Lupi, Sci. Rep. **3**, 2990 (2013).
[34] Z. Hiroi, J. Yamaura, T. Hirose, I. Nagashima, and Y. Okamoto, APL Mater. **3**, 041501 (2015).
[35] Because of the large error bars, it is difficult to discern whether the increase of the slope of ω_p^2 at 219 K is real or not. If it is real, it might come from the detailed band, i.e., nonparabolicity, because our assumption about single parabolic electron and hole bands may invalid when the bottom (top) of the conduction (valence) bands moves far away from E_F.
[36] The general Lifshitz transition can be seen as a continuous transition defined only at $T = 0$ and becomes a crossover at finite temperatures [37]. According to the original paper written by Lifshitz [24], this transition makes singularities in the second and third derivatives of thermodynamic potentials only at the zero temperature. In the finite temperature (like in $Cd_2Os_2O_7$), such singularities in all the thermodynamic properties were smeared, thereby making the Lifshitz transition a crossover.
[37] Y. Okamoto, A. Nishio, and Z. Hiroi, Phys. Rev. B **81**, 121102(R) (2010).
[38] S. Uchida, T. Ido, H. Takagi, T. Arima, Y. Tokura, and S. Tajima, Phys. Rev. B **43**, 7942 (1991).
[39] http://elk.sourceforge.net.
[40] C. Ambrosch-Draxl and J. O. Sofo, Comput. Phys. Commun. **175**, 1 (2006).